The expected low field magnetocaloric effect of $La_{0.7}Ba_{0.3}MnO_3$ manganite at room temperature.

Abd El-Moez A. Mohamed[1,2*], B. Hernando[2]

[1] Physics Department, Faculty of Science, Sohag University, Sohag 82524, Egypt

[2] Physics Department, Faculty of Science, Oviedo University, Oviedo 33007, Spain

Abstract

$La_{0.7}Ba_{0.3}MnO_3$ manganite oxide was prepared by the sol-gel method. X-ray diffraction has shown the high homogeneity of the compound and Reitveld refinement has proved the R-3C rhombohedral structure. The temperature dependence of magnetization at different applied magnetic fields of 50 Oe, 100 Oe and 200 Oe shows a magnetic phase transition at room temperature around 302K. The magnetocaloric properties and the related parameters have been calculated theoretically based on a phenomenological model. The results include the magnetic field dependence of magnetic entropy change, relative cooling power and specific heat. The constructed universal curve of the magnetic entropy change has proved the second order nature of magnetic phase transition in the studied compound.

Keywords: Magnetization; Phenomenological model; Magnetocaloric effect; Universal curve.

* Corresponding author: TEL/Fax: +34985105310/+34985103324

Email address: abdmoez_hussien@science.sohag.edu.eg

1. Introduction

Magnetic refrigeration based on magnetocaloric effect (MCE) phenomenon is a green energy technique in cooling technology compared with the traditional gas compression mode. This phenomenon belongs to magnetic materials and refers to the magnetic entropy change (ΔS) due to magnetic field application. The applicable

magnetocaloric materials should interest with high ΔS response in a wide temperature range. Gd [1] and its based alloys [2] are considered promising MCE materials in spite of the high cost that hinders their usage. This has increased the interest to investigate alternative magnetic materials for MCE applications as the ferromagnetic doped manganites $A_{1-x}B_xMnO_3$ (A is rare earth element and B is divalent ion). Doped manganites are low cost materials characterized with their simple preparation methods. The MCE of manganites has been discussed previously in several works that have shown the well MCE response of these compounds around their Curie temperature (T_c) [3]. For example, $La_{0.6}Ca_{0.4}MnO_3$ compound shows a MCE response of 5.27 J/kg.K at 1.5 T that is comparable with low field MCE of Gd results [4]. Also, *B. Arayedh et al* [5] have shown the enhancement of MCE of $La_{0.7}Sr_{0.3}MnO_3$ compound with the partial substitution in Mn-site by other ions as Sn, Ti and Cr, where, the MCE response showed the values of 0.47, 1.45 and 1.76 J/kg.K for these ions, respectively. Another attempt trying the effect of annealing process on the MCE has been made by *A. A. Mohamed et al* [6], where, the MCE of $La_{0.7}Ba_{0.3}MnO_3/TiO_2$ showed a notable enhancement with annealing temperature. The electro-magnetic properties of doped manganites are highly dependent on ionic size mismatch and on doping level (x), which are controlling the double exchange interaction (DE) between Mn^{3+}/Mn^{4+} ions [7] and structure symmetry. The small difference in ionic size between La^{3+} and Ba^{2+} makes La^{3+}partial substitution an interesting topic in $LaMnO_3$ compound. Such substitution enhances structural and elctro-magnetic properties of $LaMnO_3$ compound that makes $La_{0.7}Ba_{0.3}MnO_3$ a fruitful compound for investigation [8].

The interest in environmental friendly MCE applications has motivated also the theoretical studies to explain the MCE properties of magnetic materials [9-12]. For example, the MCE properties of $ErCo_2$ and $Er_{0.8}Y_{0.2}Co_2$ compounds have been explained

theoretically considering the localized and the itinerant magnetic contribution to the entropy [13]. In addition, some phenomenological models have been established to expect the best MCE properties of materials [11]. So, in this work we trying to tailor the room temperature low field MCE of $La_{0.7}Ba_{0.3}MnO_3$ compound using a phenomenological model reported in Ref. [11].

2. Experimental method

$La_{0.7}Ba_{0.3}MnO_3$ manganite was prepared by the sol-gel route as reported in Ref. [14] with 1150°C sintering temperature. Crystal structure was examined by x-ray diffraction (XRD) at room temperature, and structural analysis was performed with Rietveld refinement method using FULLPROF program. The magnetization dependence on temperature was measured at 50 Oe, 100 Oe and 200 Oe applied magnetic fields.

3. Results and discussion

3.1. Structure

Fig. 1 shows the room temperature XRD pattern of $La_{0.7}Ba_{0.3}MnO_3$ manganite compound. The pattern exhibits the absence of impurity phases revealing the high homogeneity of the compound. The structural analysis using Reitveld refinement shows the R-3c rhombohedral structure, and the inset of Fig. 1 displays profile refinement, where the red points are the experimental data, the black points are the calculated data, the blue line is the difference between them and the green ticks are Bragg positions.

3.2. Magnetocaloric modeling investigation

The comprehensive investigation of MCE includes studying some parameters besides ΔS values as the full width at half maximum of ΔS curve (δT_{FWHM}), the relative cooling power (RCP) and the specific heat (ΔC_p) change. The used theoretical approach requires the experimental values of $\mathbf{M_i}$, $\mathbf{M_f}$, $\mathbf{T_c}$, $\mathbf{B}$ and $\mathbf{S_c}$ listed in Table 1. Where, $\mathbf{M_i}$ is an

initial magnetization value at $\mathbf{T_i}$ temperature ($T_i < T_c$), $\mathbf{M_f}$ is a final magnetization value at $\mathbf{T_f}$ temperature ($T_f > T_c$), **B** is the dM/dT at $\mathbf{T_i}$ and $\mathbf{S_c}$ is the dM/dT at T_c.

Open circles in Fig. 2 represent the experimental results of the magnetization dependent temperature, M(T), at different applied magnetic fields. The hyperbolic ferromagnetic-paramagnetic transition (FM-PM) characterizes $La_{0.7}Ba_{0.3}MnO_3$ compound at T_c=302K, which is a common transition shape in manganites oxides, in agreement with [12, 15]. It is noteworthy also the increase in magnetization value with increasing the applied magnetic field. The ferromagnetism below T_c refers to the DE interaction between Mn^{3+} and Mn^{4+} (Mn^{3+}-O-Mn^{4+}), which is enhanced with the applied magnetic field leading to the increase in magnetization value. Whereas, the paramagnetism above T_c is attributed to the spins disorder as a result of temperature increase. According to the used phenomenological model, M(T) has been generated using Eq.1 and represented by the solid lines in Fig.2, where, $\mathbf{A}=\frac{2(B-S_c)}{M_i-M_f}$ and $\mathbf{C}=\frac{M_i+M_f}{2}+\mathbf{B}T_c$. The large agreement between experimental and theoretical results of M(T) in Fig. 2 reveals the accuracy of the present model.

$$\mathbf{M}=\left(\frac{M_i-M_f}{2}\right)\tanh\left[\mathbf{A}\left(T_c-T\right)\right]+\mathbf{B}T+\mathbf{C} \quad (1)$$

$$\Delta S=\left\{-A\left(\frac{M_i-M_f}{2}\right)\ sech^2\left[A(T_c-T)+B\right]\right\}H \quad (2)$$

$$\delta T_{FWHM}=\frac{2}{A}\,\mathrm{sech}\left[\sqrt{\frac{2A(M_i-M_f)}{A(M_i-M_f)+2B}}\right] \quad (3)$$

$$RCP=\left(M_i-M_f-2\frac{B}{A}\right)H\ \mathrm{sech}\left[\sqrt{\frac{2A(M_i-M_f)}{A(M_i-M_f)+2B}}\right] \quad (4)$$

The temperature dependence of ΔS at different applied magnetic fields has been calculated using Eq. 2 and is displayed in Fig. 3, where it shows a ΔS maximum (ΔS_{max}) around T_c with magnetic field dependence. ΔS arises from magnetic spin order/disorder feature, where, magnetic field application aligns spins that decreases their spin entropy. This explains the constant behavior of ΔS at low temperatures due to the ferromagnetic spin ordering. Around T_c, the FM-PM transition increases the magnetic spins-disorder that reaches maximum at T_c resulting in ΔS_{max}. The values of δT_{FWHM} has been obtained from Eq. 3, it increases systematically with the applied magnetic field as shown in Table 2. Depending on ΔS_{max} and δT_{FWHM} values, the magnetocaloric efficiency can be determined through the RCP [16], which pointing to the transferred heat between the cold and the hot reservoirs in a refrigerator during one ideal thermodynamic cycle [17]. The calculated values of RCP have been given by Eq. 4, which are increasing linearly with the applied magnetic field as listed in Table 2. The increase in RCP with the applied magnetic field is reasonable due to the proportional relation between ΔS& δT_{FWHM} and the applied magnetic field. According to this proportional relation, we can expect the saturation for ΔS and RCP at large applied magnetic fields due to the magnetic moment saturation (M(T)) at these high magnetic fields.

The temperature dependence of ΔC_p at different applied magnetic fields has been calculated using Eq.5 and shown in Fig. 4. As observed, ΔC_p shows a crossover from negative minimum $\Delta C_{P,H(min)}$ to positive maximum $\Delta C_{P,H(max)}$ values at T_c due to the magnetic phase transition [18] accompanied by a monotonic increase in the minimum/maximum ΔC_P values with the applied magnetic fields (see Table 2).

$$\Delta C_{p,H} = -AT^2(M_i-M_f).Sech^2\,[A(T_c-T)]\,.\,\tanh\,[A(T_c-T)].H \qquad (5)$$

$$\theta = -(T-T_c)/(T_L-T_c) \quad \text{for } T \leq T_c \qquad (6)$$

$$\theta = (T-T_c)/(T_R-T_c) \quad \text{for } T > T_c \qquad (7)$$

The universal curves of magnetic entropy, $S_R(\theta)$, is one of methods used to determine the nature of the FM-PM transition. The universal curves in Fig.3 have been built using $S_R = \Delta S(T)/\Delta S_{max}$ relation, and the rescaled temperature **θ** has been constructed using Eq. 6 and Eq. 7, where, $\mathbf{T_L}$ and $\mathbf{T_R}$ are reference temperatures satisfying $\Delta S(T)/\Delta S_{max}=0.5$ [19]. Data points in the universal curves collapse with each other revealing the universal behavior that confirms the second order transition [20]. As a second order transition, ΔS is supposed to obey the exponent power law $\Delta S=a(\mu_0 H)^n$ [21], where ***a*** is a constant and ***n*** is an exponent power depending on sample's magnetic state. The fitting of this equation in Fig. 6 has shown the 1.2 value for ***n*** at T_c, which is very far from the mean field theory predicted value (n=0.67) [21] referring to the local inhomogeneity or the superparamagnetic clusters near T_c [22, 23].

4. Conclusion

$La_{0.7}Ba_{0.3}MnO_3$ manganite with R-3c rhombohedral structure was prepared using the sol-gel method. The magnetization measurement has shown the FM-PM transition in the room temperature range at T_c=302K. The magnetocaloric properties at low magnetic field change of 50 Oe, 100 Oe and 200 Oe have been predicted using a phenomenological model. The MCE increases monotonically with the applied magnetic field, for example, the RCP reaches $13x10^{-3}$, $50\ x10^{-3}$ and $189\ x10^{-3}$ J/kg at 50 Oe, 100 Oe and 200 Oe respectively. Moreover, the FM-PM transition for $La_{0.7}Ba_{0.3}MnO_3$ manganite has been classified as a second order nature of magnetic transition according to the constructed universal curve.

Acknowledgment

This work was financially supported by the Spanish Economy Department Ref. MAT201347231-C2-1-P and MAT2013-48054-C2-2-R, by the Asturias Government Ref. FC-15-GRUPIN14-085 research projects and authors would like to acknowledge the Egyptian Ministry of Higher Education.

References

1- V. K. Pecharsky, K. A. Gschneidner Jr., J. Magn. Magn. Mater. 167 (1997) L179.

2- V. K. Pecharsky, K. A. Gschneidner Jr., Phys. Rev. Lett. 78 (1997) 4494.

3- S. Kallel, N Kallel, O. Pena, M Oumezzine, Mater. Lett. 64 (2010) 1045.

4- J.C. Debnath, R. Zeng, J.H. Kim, S.X. Dou, J. Appl. Phys. 107 (2010) 09A916.

5- B. Arayedh, S. Kallel, N. Kallel, O. Pe~na, J. Magn. Magn. Mater. 361 (2014) 68.

6- A. A. Mohamed, V. Vega, M. Ipatov, A.M. Ahmed, B. Hernando, J. Alloy Compd. 665 (2016) 394.

7- C. Zener. Phys. Rev. 81 (1951) 440.

8- C. P. Reshmi, S. S. Pillai, K. G. Suresh, M. R. Varma, Solid State Sci. 19 (2013) 130.

9- P. J. Von Ranke, N.A. de Oliveira, S. Gama, Phys. Lett. A 320 (2004) 302.

10- P. J. Von Ranke, N. A. de Oliveira, C. Mello, A. Magnus, G. Carvalho, S. Gama, Phys. Rev. B 71 (2005) 054410.

11- M. A. Hamad. Phase Transit. 85 (2012) 106.

12- K. Raju, N. P. Kumar, P. V. Reddy, D. H. Yoon, Phys. Lett. A 379 (2015) 1178.

13- N. A. de Oliveira, P. J. von Ranke, M. V. Tovar Costa, A. Troper, J. Appl. Phys. 91(2002) 15.

14- N. A. Shah, P. S. Solanki, R. Ashish, D. G. Kuberkar, Appl. Nanosci 5 (2015) 135.

15- A. A. Mohamed, V. Vega, M. Ipatov, A.M. Ahmed, B. Hernando, J. Alloy Compd. 657 (2016) 495.

16- J. Mira, J. Rivas, L. E. Hueso, F. Rivadulla, M. A. L.Quintela, J. Appl. Phys. 91 (2002) 8903.

17- M. H. Phan, S. C.Yu, J. Magn. Magn. Mater. 308 (2007) 325.

18- H. Yang, Y. H. Zhu, T. Xian, J. L. Jiang, J. Alloys Compd. 555 (2013) 150.

19- V. Franco, J.S. Blazquez, B. Ingale, A. Conde, Annu. Rev. Mater. Res. 42 (2012) 305.

20- V. Franco, J. S. Blazquez, A. Conde, J. Appl. Phys. 103 (2008) 07B316.

21- H. Oesterreicher, F. T. Parker, J. Appl. Phys. 55 (1984) 4334.

22- V. Franco, J. S. Blazquez, A. Conde, Appl. Phys. Lett. 100 (2006) 064307.

23- V. Franco, J. S. Blazquez, A. Conde, Appl. Phys. Lett. 89 (2006) 222512.

Table 1 Model parameters at 50 Oe, 100 Oe and 200 Oe of $La_{0.7}Ba_{0.3}MnO_3$ compound.

μ_0H (Oe)	M_i (emu/g)	M_f (emu/g)	T_c (K)	B (emu/g.K)	Sc (emu/g.K)
50	5.74	0.0131	302	-0.00046	-0.17
100	11.057	0.026	302	-0.00289	-0.294
200	20.78	0.053	302	-0.0048	-0.474

Table2 The expected values of magnetocaloric properties for $La_{0.7}Ba_{0.3}MnO_3$ compound at different applied magnetic fields.

μ_0H (Oe)	ΔS_{max}(J/kg.K) $x10^{-3}$	δT_{FWHM} (K)	RCP (J/kg) $x10^{-3}$	$\Delta C_{P,H\ (max)}$ (J/kg.K) $x10^{-3}$	$\Delta C_{P,H\ (min)}$ (J/kg.K)$x10^{-3}$
50	0. 8	15.48	13	2	-1.9
100	3	17.26	50	3	-3
200	5	20.14	189	5	-4.4

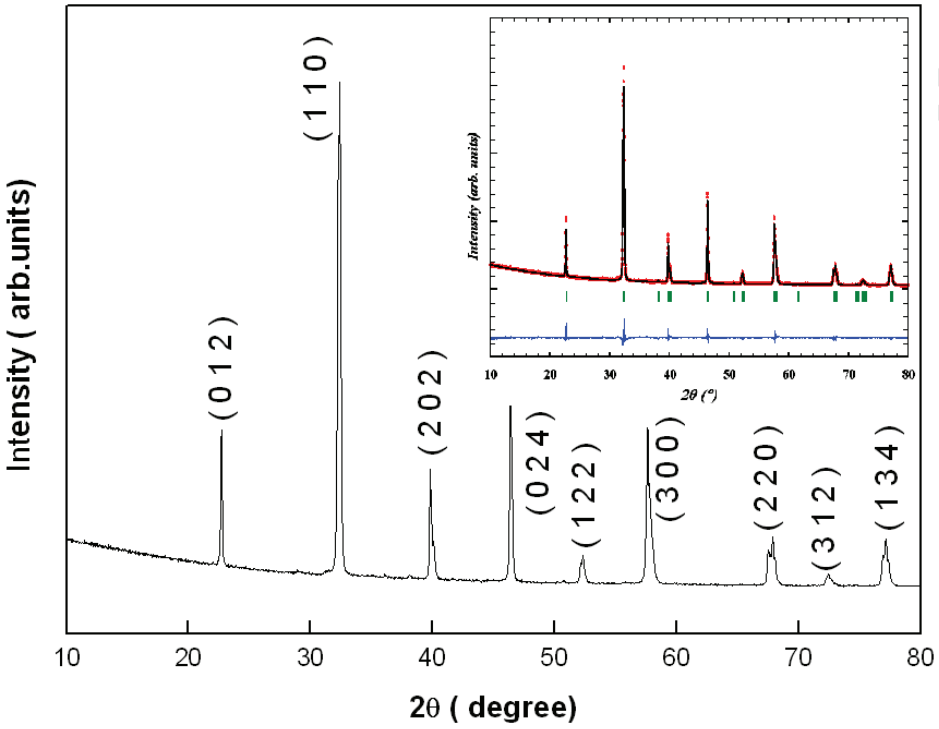

Fig. 1: XRD pattern of $La_{0.7}Ba_{0.3}MnO_3$ compound and the inset shows Reitveld refinement profile

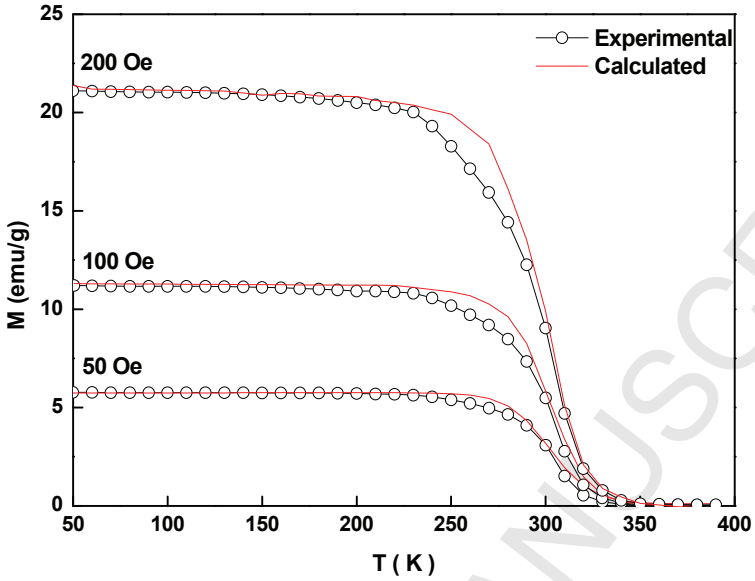

Fig. 2: The experimental and the theoretical temperature dependence of magnetization for $La_{0.7}Ba_{0.3}MnO_3$ manganite.

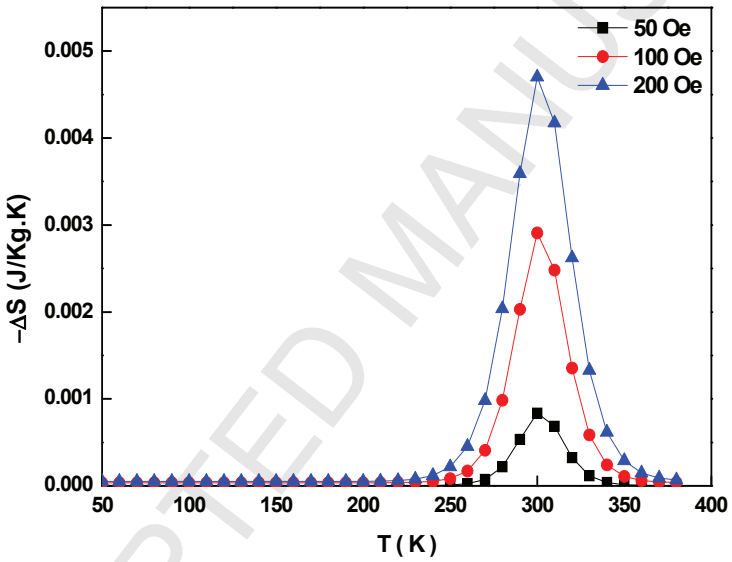

Fig. 3: Thermal variation of ΔS at different applied magnetic fields for the $La_{0.7}Ba_{0.3}MnO_3$ manganite.

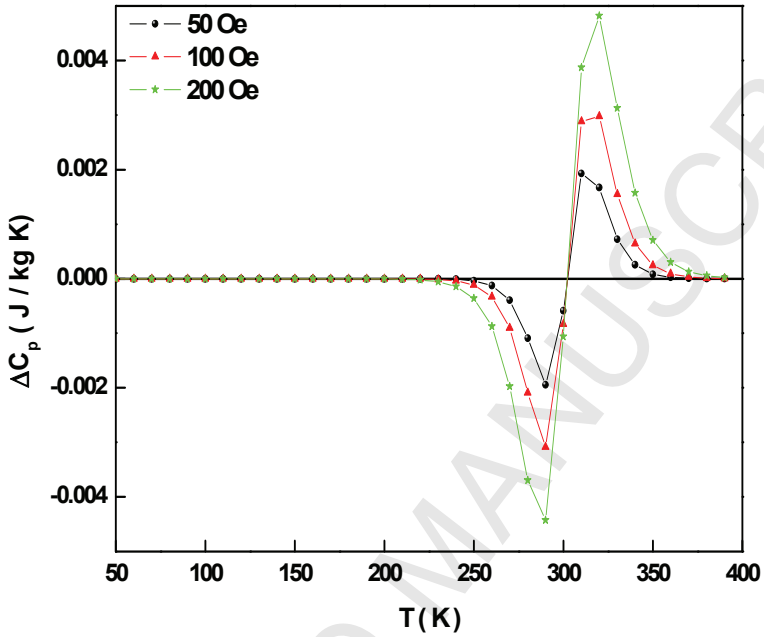

Fig. 4: The temperature dependent ΔCp at different applied magnetic fields of $La_{0.7}Ba_{0.3}MnO_3$ manganite.

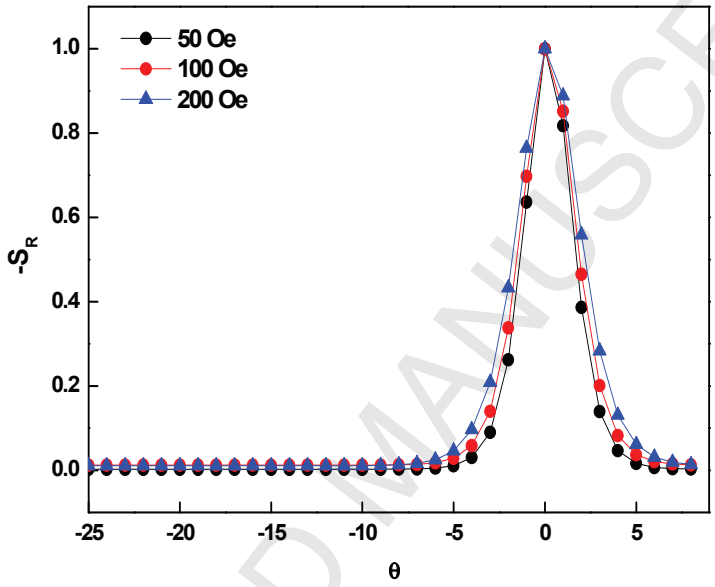

Fig. 5: The universal curves of $La_{0.7}Ba_{0.3}MnO_3$ manganite compound.

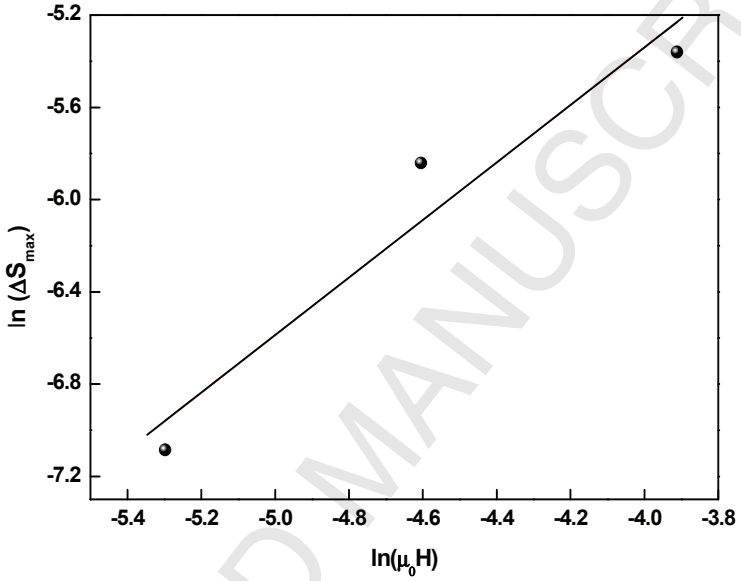

Fig. 6: ln (ΔS_{max}) vs ln ($\mu_0 H$) for $La_{0.7}Ba_{0.3}MnO_3$ compound.